

# Transparent Nanometric Organic Luminescent Films as UV-Active Components in Photonic Structures

Francisco J. Aparicio, Miguel Holgado, Ana Borrás, Iwona Blaszczyk-Lezak, Amadeu Griol, Carlos A. Barrios, Rafael Casquel, Francisco J. Sanza, Hans Sohlström, Mikael Antelius, Agustín R. González-Elipe, and Angel Barranco\*

The flavonoids, which are natural compounds in diverse plants, have been extensively studied due to their antioxidant properties in biological systems.<sup>[1]</sup> Within this family, 3-hydroxyflavone (3HF) is one of the most interesting derivatives because of its singular luminescent properties. In solution under UV illumination this molecule shows two types of fluorescence emission: a normal deep-violet emission and a yellow-green emission assigned to an excited proton transfer tautomer of the normal molecule with a large Stokes' shift of  $\approx 180$  nm. This excited state intermolecular proton transfer mechanism (ESIPT) of 3HF in solution was initially described by Sengupta and Kasha and further studied by many authors in the last decades.<sup>[2–4]</sup> This process involves a very efficient non-radiative energy dissipation mechanism in which the 3HF molecule absorbs one photon while in the excited state, one hydroxyl proton is transferred to a neighboring carbonyl group.<sup>[5]</sup> The ESIPT mechanism in 3HF is very sensitive to the chemical environment. Thus, emission of the tautomer form with a very low contribution of the normal emission has been observed in nonpolar media.<sup>[4,6,7]</sup>

The molecule in solution has been extensively utilized as colorimetric reagent, polarity probe, and probe in biological microenvironments or lasing mediums.<sup>[1,3,8]</sup> Hydroxyflavone-doped polymeric thin films prepared by solution polymerization and sol-gel hybrid films have been utilized as scintillator and wavelength shifters.<sup>[6,9]</sup> Films prepared by vacuum deposition, magnetron sputtering, and other methods have been used

in organic light-emitting diodes (OLEDs) and in commercial Si photodiodes.<sup>[9,10]</sup>

In this article, we present an alternative approach to the fabrication of 3HF-containing thin films and their unprecedented implementation as active components in photonic structures that can be useful for the fabrication of devices such as UV sensors, UV-to-visible wavelength shifters, and UV filters. In this preparation procedure, the films are deposited in vacuum at room temperature by sublimating the dye in the downstream region of a low-power microwave plasma. The main difference from a standard vacuum deposition or a plasma polymerization process is that the interaction with the plasma produces the fragmentation of only a fraction of the dye molecules in the gas phase creating highly reactive molecular moieties that form a polymeric-like film on the substrate surface.<sup>[11]</sup> In this plasma-assisted vacuum deposition process, the working conditions and reactor geometry are finely controlled to avoid a complete fragmentation of the dye molecules. The resulting material is a polymeric film with a given percentage of integer 3HF molecules embedded in it, which exhibits quite different properties than those of layers obtained by the direct sublimation of molecules. Although some examples of a similar synthetic methodology have been very recently reported for other functional molecules, this is the first time that such deposition process is applied to the growth of luminescent films from 3HF as the single precursor.<sup>[11–13]</sup> The composition of the films as determined by X-ray photoelectron spectroscopy (XPS) analysis was 78% C and 22% O. This composition is close to that corresponding to the molecular formula of the dye (i.e., 83% C and 17% O). The oxygen enrichment found on these polymeric films is a general characteristic of any deposition process involving plasmas.<sup>[11–13,15]</sup>

To characterize the films and further confirm the incorporation of integer dye molecules into the polymeric matrix we used the time of flight secondary ion mass spectrometry (ToF-SIMS) technique. Among the very numerous peaks in the spectrum shown in **Figure 1a**, the most intense ones, which appear in the region with a mass-to-charge ratio ( $m/z$ ) between 40 and 120, are associated with the cross-linked polymeric matrix. The spectrum also clearly depicts the peaks corresponding to the 3HF M+ ( $m/z \approx 238$ ) and MH+ ( $m/z \approx 239$ ) molecular ions, indicating a high percentage of integer 3HF molecules embedded in the film. This spectrum is very different from the 3HF reference spectrum (see Figure S1 in the Supporting Information), which is composed of the molecular ions peaks and a few low intense peaks at lower  $m/z$ .<sup>[14]</sup>

F. J. Aparicio, Dr. A. Borrás, Dr. I. Blaszczyk-Lezak,  
Prof. Dr. A. R. González-Elipe, Dr. A. Barranco  
Instituto de Ciencia de Materiales de Sevilla  
(CSIC-Universidad de Sevilla)  
c/Américo Vespucio 49, ES 41092 Sevilla, Spain  
E-mail: angelbar@icmse.csic.es

Dr. M. Holgado, R. Casquel, F. J. Sanza  
Centro Laser UPM, Ctra. de Valencia  
km. 7.300, 28031 Madrid, Spain

Dr. C. A. Barrios  
Instituto de Sistemas Optoelectronicos y Microtecnología  
(ISOM-UPM), Ciudad Universitaria s/n  
28040 Madrid, Spain

Dr. A. Griol  
Nanophotonics Technology Center NTC, UPLV, Camino de Vera s/n  
46022 Valencia, Spain

Dr. H. Sohlström, M. Antelius  
Microsystem Technology Lab. KTH-Royal Institute of Technology SE-100  
44 Stockholm, Sweden

DOI: 10.1002/adma.201003088

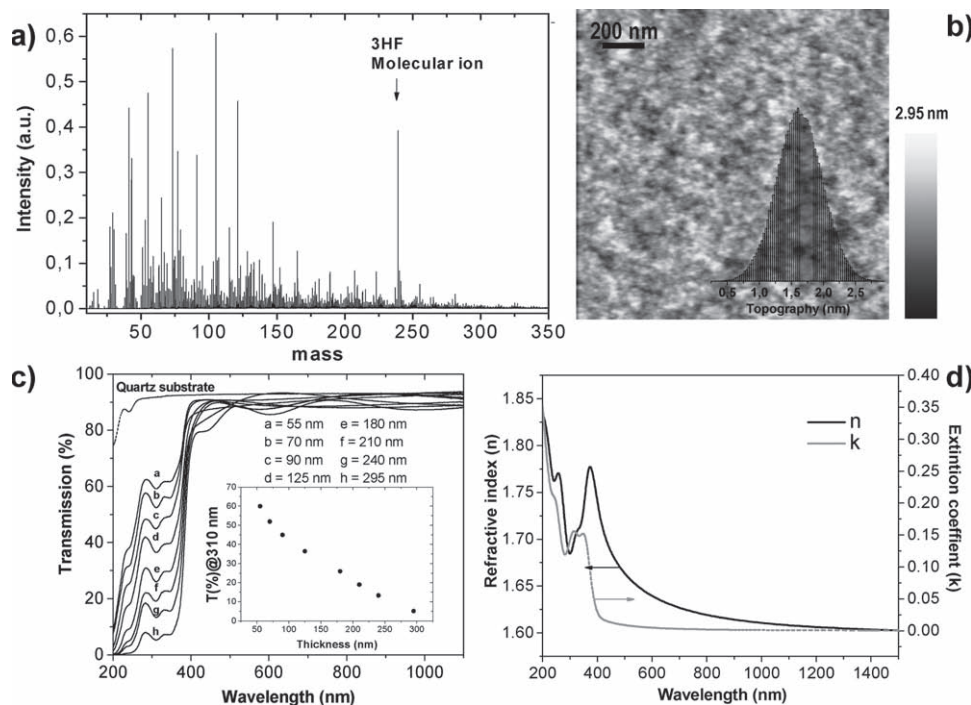


**Figure 1.** a) ToF-SIMS spectrum of a 3HF 120-nm film, b) AFM image of a 150-nm thin film, c) UV-vis transmission spectra of films with different thickness, and d) refractive index and extinction coefficient as a function of the wavelength of a  $\approx$ 100-nm thin film.

A high transmittance in the visible and a low roughness are critical requirements for the integration of the dye thin films together with photonic structures. For this application, mechanical stability and insolubility in water or alcohol are additionally required conditions that are fulfilled by the films. The atomic force microscopy (AFM) image of a 3HF thin film shown in Figure 1b confirms that the surfaces of these films are very homogeneous, crack-free, and smooth with a RMS roughness of  $\approx$ 0.4 nm. Such a low surface roughness ensures that there will be no significant light scattering at the surface of the films incorporated onto the photonic structures. The absence of any light dispersing crystalline aggregates, typically found in other dye sublimated films, is another remarkable feature of the 3HF films evident by optical characterization.<sup>[13,17]</sup>

Figure 1c shows the UV-vis transmission spectra of a set of 3HF thin films with different thicknesses. All the films absorb in the UV region and are transparent in the visible region (i.e.,  $\lambda > 390$  nm), a significant property for many final applications of these films.<sup>[18]</sup> The absorption features at  $\approx$ 310 and  $\approx$ 345 nm are similar to those reported for dilute alcoholic solutions of the dye.<sup>[1,4]</sup> The intense and continuous light absorption at wavelengths lower than 390 nm can be attributed to both the dye molecules and the unsaturated bonds in the polymeric matrix. It is also worth noting the high UV absorption capacity of films with a thickness as low as  $\approx$ 50 nm and the fact that for  $\approx$ 300 nm films UV absorption is nearly complete. Saturation of absorption and the sharpness of the absorption edge are requirements for the fabrication of UV filters, an application where these films can compete in performance with thin-film materials prepared by other methods.<sup>[19]</sup> At wavelengths higher than  $\approx$ 390 nm, i.e., the visible and near infrared regions, the films are

visible blind (transparent) showing the typical interference patterns due to having a different refractive index than the substrate (Figure 1c). The high transparency of these films in the entire visible range is confirmed by the very low value of its extinction coefficient function determined by ellipsometry (Figure 1d). The refractive index value of the 3HF thin films is 1.62 at 630 nm.

The fluorescence behavior of the 3HF polymeric films is analyzed in Figure 2. The shape of the excitation spectrum in Figure 2a, characterized by a maximum at  $\approx$ 345 nm and a shoulder at  $\approx$ 310 nm, is very similar to that of the dye molecule in solution.<sup>[1,4]</sup> Information about the corresponding fluorescence intensity decay can be found in the Supporting Information (Figure S2). The emission spectrum is formed by a single and intense feature at  $\approx$ 535 nm, corresponding to the tautomer emission of the 3HF molecule. Meanwhile, the emission of the normal form at  $\approx$ 425 nm is negligible. This result suggests that the nonpolar character of the cross-linked 3HF polymeric matrix quenches the hydrogen bond donating ability of the molecule.<sup>[4,9]</sup> From the point of view of their applications, it also sustains the use of these materials as selective emitters of green light or as UV detectors since, contrary to the molecule in solution or other media, only one emission channel remains in the films. To prove the feasibility of this latter application, Figure 2b shows that the fluorescence emission varies almost linearly with the UV light ( $\lambda = 360$  nm) for a large range of intensities (i.e., 0.01–1.5 mW cm<sup>-2</sup>). No departures from this linear behavior are observed after several cycles of increasing and decreasing the UV irradiation, thus demonstrating the high UV stability of the films. The emission process has to be very intense for this application and for its potential use as green light emitter.

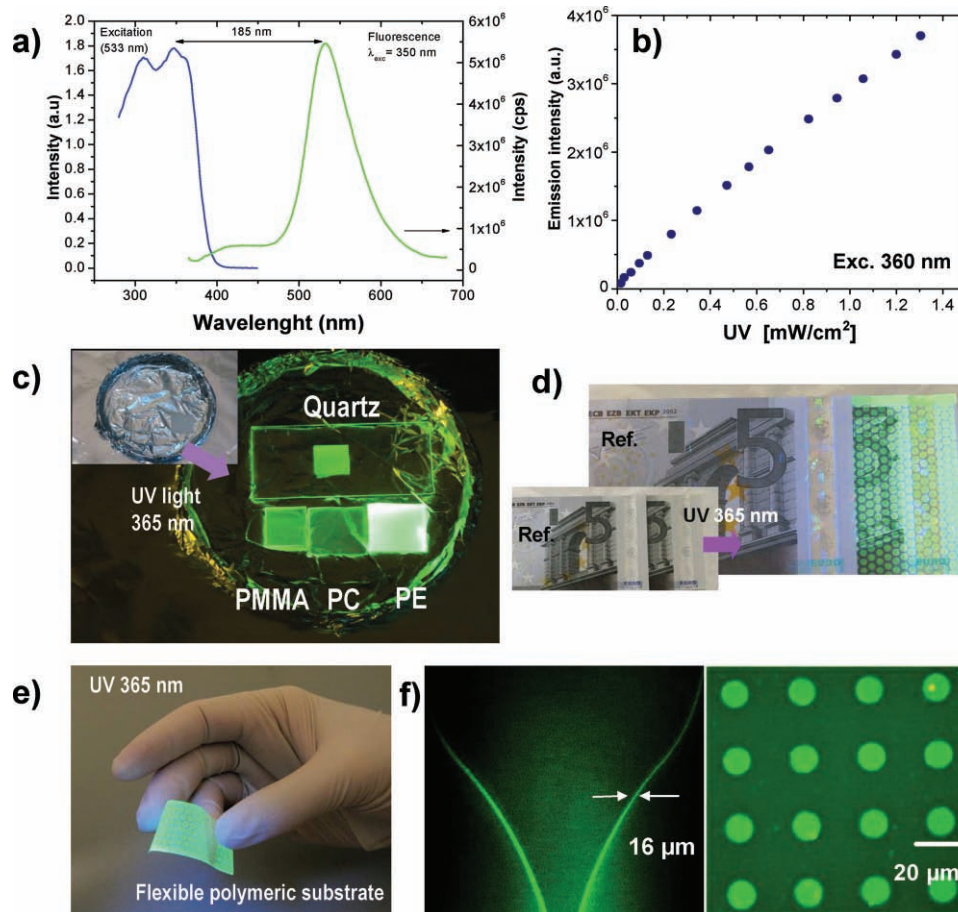


**Figure 2.** a) Excitation and emission spectra of an  $\approx 100$ -nm-thick thin film, b) evolution of the intensity of the emission spectrum as a function of the UV intensity used for excitation, c–e) photographs of a series of transparent luminescent thin films deposited onto several sensitive substrates as labeled, and f) fluorescence microscopy images taken of 3HF films deposited through masks designing a squared pattern and two lines of a waveguide structure.

This is shown in Figure 2c, where the green light emitted by the films that are illuminated with a low intensity UV lamp (see illuminated walls of the container) can be easily observed with the naked eye. The experiments in this figure corresponds to a  $\approx 100$ -nm-thick film deposited on glass, polyethylene, PMMA, and polycarbonate, both before and during UV illumination. Two additional examples of the deposition onto Euro bank notes and a flexible polymer are also included (Figure 2d,e) to demonstrate the full compatibility of the deposition process with any kind of sensitive substrate. These examples also prove the high efficiency for green light emission, which is clearly appreciable even under daylight conditions. Another advantage of this methodology is the straightforward lithographic deposition of the thin films in one step. The fluorescence microscopy images in Figure 2f show a micrometric pattern and a planar waveguide-like pattern obtained by the deposition of an  $\approx 100$ -nm film through a shadow mask. The possibility of depositing optical structures using masks, together with the mechanical, optical, and luminescent properties of the 3HF polymeric films, make them ideal for incorporation as active materials in photonic structures (i.e., interferometric and resonant structures) used for the fabrication of photonic devices. Furthermore,

the 3HF polymeric films can be selectively removed from the surface by plasma etching, which ensures that the photonic structures, the most expensive part of the final devices, can be reused for the preparation of new devices.

Three different photonic structures incorporating the fluorescent films are presented here to demonstrate the feasibility of this concept: a vertical and a planar Fabry–Perot (F–P) resonator and a disk resonator. The vertical F–P resonator structure is relatively simple and consists of a periodic 1D photonic crystal with a central planar defect. The 3HF dye thin film is the active component and is deposited as the upper cladding of the multilayered structure (see the schematic of the device in the Supporting Information, Figure S3 A1–2). The periodic distribution of thin layers, forming a Bragg reflector, consists of 18 pairs of nine  $\text{SiO}_2$  (100 nm) and  $\text{Si}_3\text{N}_4$  (65 nm) layers, while the defect or cavity is a  $\text{Si}_3\text{N}_4$  thin film of 190 nm. The structure is designed to have a wide photonic band gap extending from 460 to 625 nm with a sharp transmission peak with a full width at half-maximum (FWHM) of  $\approx 2.5$  nm located at  $\approx 535$  nm within the spectral position of the 3HF polymer fluorescence maximum (see structure VC18 in Figure 3,A1). Figure 3,A2 shows the emission spectrum of a 3HF thin film deposited on

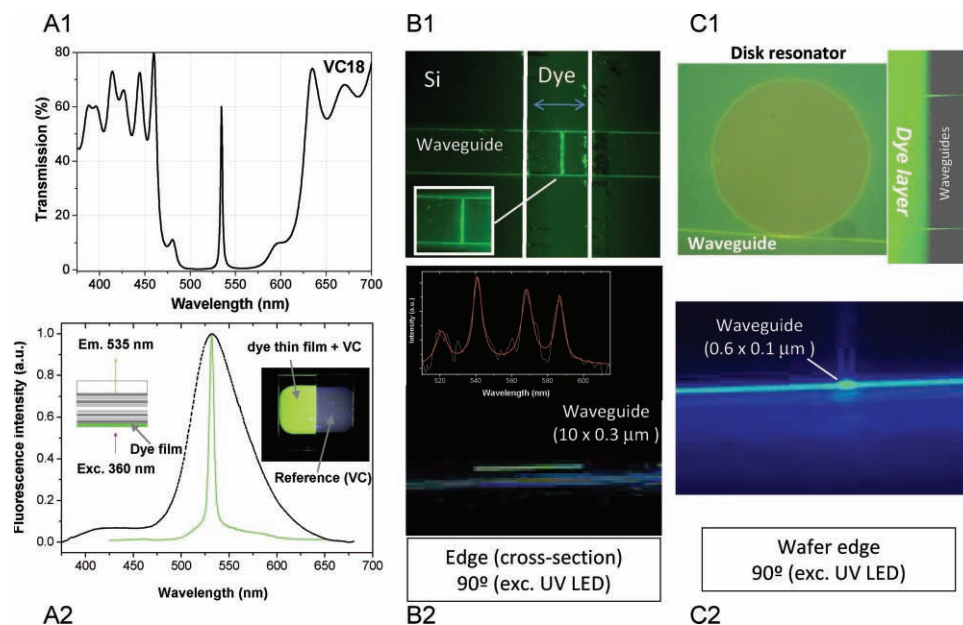


**Figure 3.** Responses of the 3HF thin film deposited onto photonic structures. A1) Transmission spectrum through a vertical cavity and A2) comparison of the fluorescent spectra recorded for a 3HF film deposited on a quartz slice and onto the vertical cavity, measured as indicated in the insets. B1) Normal fluorescence microscopy images of a F–P structure with the 3HF film deposited on the resonator zone. B2) Fluorescence image taken in cross section at the edge of the output waveguide. The inset shows the experimental and fitted (red line) transmission modes obtained of the fluoresce emission modulated by the F–P resonant cavity. C1) Normal fluorescence microscopy images taken for a ring resonator structure with the 3HF film deposited on the resonator zone and from a boundary zone showing the fluorescence light carried by two wave guides. C2) Picture of the end part of the waveguide at the wafer edge.

quartz and the same spectrum measured through the vertical structure where the 3HF thin film was deposited as a cladding. The plot shows that the fluorescence light of the dye layer is converted from a relatively broad band with a FWHM of  $\approx 65.8$  nm to a peak with a FWHM of  $\approx 3.5$  nm when transmitted through a structure whose surface is illuminated with UV light. A picture of the transmitted fluorescence light is shown in the inset of the Figure 3,A2.

The second photonic structure is based on a silicon nitride multimode strip waveguide with a width of  $10 \mu\text{m}$  and a height of  $300$  nm. The lower cladding is a  $5\text{-}\mu\text{m}$ -thick  $\text{SiO}_2$  layer grown on Si. The planar F–P resonator consists of  $\text{Si}_3\text{N}_4/\text{air}$  pairs separated  $90$  nm with a cavity height of  $140$  nm (see Supporting Information, Figure S3,B2). The dye layer was selectively deposited through a mask, only onto the resonant microcavities (see Supporting Information, Figure S3,B1). The waveguide and resonator structure are designed to transmit the 3HF emission up to the output, even if there are several transmission modes. Figure 3,B1 shows a fluorescence microscopy image of the 3HF active area covering the resonator structure, while Figure 3,B2 shows a fluorescence confocal image taken in cross section to prove that the fluorescence light is selectively transmitted through the wave guide. In the inset of this figure it can be observed that the transmission modes of the fluorescence emission are modulated by the F–P resonant cavity at the edge of the output waveguide.

The third photonic structure consisted of a disk resonator and a  $\text{Si}_3\text{N}_4$  strip forming a high refractive index waveguide (Supporting Information, Figure S3,C1,C2). The waveguide cross section was  $600$  nm and its height was  $\approx 80$  nm, a topology

that only permits the propagation of the fundamental transverse electric (TE) mode. The lower cladding was a layer of  $\text{SiO}_2$  with a thickness of  $5 \mu\text{m}$  on a Si substrate. The upper cladding was also  $\text{SiO}_2$ . A window through this  $\text{SiO}_2$  upper cladding was open over the resonant disk and nearby waveguide to enable that the active 3HF film is selectively deposited onto this zone (see Figure 3,C1). In this case, the luminescent films deposition process was carried out at wafer scale covering trough masks a large number of ring resonators. The design and dimension of this photonic structure is such that the waveguide can couple the green fluorescence emitted by the active 3HF film. The disk is an optical resonator coupled by evanescent field to the waveguide. To obtain an effective coupling, the distance between the ring and the waveguide was between  $100$  and  $150$  nm and various disks with different diameters ranging from  $50$  to  $200 \mu\text{m}$  were fabricated onto a wafer. Figure S3,C2 (Supporting Information) shows a scanning electron microscopy (SEM) image of one of the disk resonator/waveguide ensembles and Figure 3,C1 shows a fluorescence microscopy image showing a device illuminated with  $\lambda \approx 365$  nm. It must be noted that the central region, including part of the strip waveguide and the whole resonant disk, is brighter than the rest of the chip. The good performance of this photonic device can be seen in Figure 3,C2, which shows that the green light is collected and transmitted up to the waveguide output in the chip edge. This preferential distribution of the fluorescence light supports the conclusion that, as predicted by electric field simulations (data not shown), the field intensity is higher in the disk and is transmitted through the waveguide out of the 3HF-coated region up to the border of the structure.

In this work a new kind of photonic organic thin film material prepared by a novel plasma-assisted vacuum deposition procedure was presented. The films consist of a polymeric matrix with a high concentration of free 3HF molecules, which absorb in the UV and emit in the visible wavelength range. Besides the extraordinary good performance as UV filter, UV sensor, and green emitter, the deposition of these films through masks onto the surface of different photonic structures has proven their suitability as photonic active components for the fabrication of reusable photonic chips. These concepts have been proven by monitoring the spectral response of a chip consisting of a vertical and planar F-P structure and by the direct observation of the fluorescence light paths in planar photonic structures (horizontal F-P and ring resonators). In the latter cases, the selective deposition through masks is another key characteristic that enables the wafer-scale fabrication of complex photonic chips. Furthermore, the deposition process allows the fabrication of the luminescent films on sensitive substrates. An outstanding achievement of the process is the direct deposition of luminescent nanometric films or patterns on flexible polymers and paper. Such advantages will be determinant for the integration of this new material as active component in organic optical and microelectronic devices.

## Experimental Section

**Plasma procedure:** The polymerized thin films were prepared by sublimation of the 3HF dye molecules (Sigma-Aldrich Co, USA) in the downstream region of the Ar microwave electron cyclotron resonance (ECR) plasma operating at 150 W at  $1 \times 10^{-2}$  mbar argon pressure. The film thickness (in the range 30–300 nm) and evaporation rate were monitored by using a quartz crystal monitor placed beside the sample holder in the deposition region (see also Refs. [11,12]). By adjusting the plasma condition and geometry of the deposition process, it was possible to reproducibly control the concentration of integer 3HF molecules in the films.

**Thin film and photonic structure characterization:** The mass spectra of the samples were recorded on a TOF-SIMS IV instrument from Ion-ToF GmbH (Germany). UV-vis transmission spectra were recorded using a Perkin-Elmer  $\lambda 12$  spectrophotometer. Fluorescence spectra were measured with a Fluorolog3 spectrofluorometer from Horiba Jobin-Yvon (Japan). Fluorescence microscopy images were obtained using a TCS SP2 confocal fluorescence microscope from Leica Microsystems (Germany). For the cross-sectional images the samples were illuminated with a 365-nm, 3-mW LED source.

Optical characterization of the thin films was been carried out using a variable angle spectroscopic ellipsometer (VASE) from J. A. Woollam Co., Inc (USA). The spectral range was 200–2000 nm and the measurements were performed at 60°, 65°, and 70° angles of incidence. Noncontact AFM measurements were carried out with a Cervantes AFM system from NANOTEC Electronica (Spain). Field emission scanning electron microscopy (FESEM) images were obtained using a Field Emission S-5200 Microscope from Hitachi (Japan).

## Supporting Information

Supporting Information is available from the Wiley Online Library or from the author.

## Acknowledgements

We thank the EU (PHODYE contract n° 033793); Projects CDS2008–0023, MAT2010–21218, and P09-TEP-5283; Dr. Carmen Serra (CACTI (University of Vigo, Spain)) for the ToF-SIMS characterization; and Dr. Alicia Orea (IBVF-CSIC-US, Seville, Spain).

Received: August 25, 2010

Revised: October 17, 2010

Published online: December 15, 2010

- [1] A. C. Boudet, J. P. Cornard, J. C. Merlin, *Spectrochim. Acta, Part A* **2000**, *56*, 829.
- [2] P. K. Sengupta, M. Kasha, *Chem. Phys. Lett.* **1979**, *68*, 382.
- [3] P. Chou, D. McMorrow, T. J. Aartsma, M. Kasha, *J. Phys. Chem.* **1984**, *88*, 4596.
- [4] A. J. G. Strandjord, P. F. Barbara, *J. Phys. Chem.* **1985**, *89*, 2355.
- [5] M. Zayat, P. Garcia-Parejo, D. Levy, *Chem. Soc. Rev.* **2007**, *36*, 1270.
- [6] J. R. Dharia, K. F. Johnson, J. B. Schelenoff, *Macromolecules* **1994**, *27*, 5167.
- [7] A. Quaranta, S. Carturan, G. Maggioni, R. Ceccato, G. Della Mea, *J. Non-Cryst. Solids* **2003**, *322*, 1.
- [8] A. S. Klymchencko, A. P. Demchenko, *J. Am. Chem. Soc.* **2002**, *124*, 12372.
- [9] a) S. Carturan, A. Quaranta, G. Maggioni, M. Bonafini, G. Della Mea, *Sens. Actuators A* **2004**, *113*, 288; b) G. Maggioni, S. Carturan, A. Quaranta, A. Patelli, G. Della Mea, *Chem. Mater.* **2002**, *14*, 4790.
- [10] Y. Hamada, T. Sano, H. Fujii, Y. Nishio, H. Takahashi, K. Shibata, *Appl. Phys. Lett.* **1997**, *71*, 3338.
- [11] A. Barranco, F. Aparicio, A. Yanguas-Gil, P. Groening, J. Cotrino, A. R. González-Elipe, *Chem. Vap. Deposition* **2007**, *13*, 319.
- [12] A. Barranco, P. Groening, *Langmuir* **2006**, *22*, 6719.
- [13] I. Blaszczyk-Lezak, F. J. Aparicio, A. Borrás, A. Barranco, A. Álvarez-Herrero, M. Fernández-Rodríguez, A. R. González-Elipe, *J. Phys. Chem. C* **2009**, *113*, 431.
- [14] NIST Chemistry WebBook database, <http://webbook.nist.gov/chemistry> (accessed August 2010).
- [15] H. Yasuda, *Luminous Chemical Vapor Deposition and Interface Engineering*, Marcel-Dekker, New York **2004**.
- [16] *Advanced Plasma Technology*, (Eds: R. d'Agostino, P. Favia, Y. Kawai, H. Ikegami, N. Sato, F. Arefi-Khonsari), Wiley-VCH, Weinheim, Germany **2008**.
- [17] F. J. Aparicio, A. Borrás, I. Blaszczyk-Lezak, P. Gröning, A. Álvarez-Herrero, M. Fernández-Rodríguez, A. R. Gonzalez-Elipe, A. Barranco, *Plasma Processes Polym.* **2009**, *6*, 17.
- [18] H. W. Lin, S. Y. Ku, H. C. Su, C. W. Huang, Y. T. Lin, K. T. Wong, C. C. Wu, *Adv. Mater.* **2005**, *17*, 2489.
- [19] P. Garcia Parejo, M. Zayat, D. Levy, *J. Mater. Chem.* **2006**, *16*, 2165.